nature ecology & evolution

SUPPLEMENTARY INFORMATION

DOI: 10.1038/s41559-017-0221-8

In the format provided by the authors and unedited.

General ecological models for human subsistence, health and poverty

Calistus N. Ngonghala[1]*, Giulio A. Leo[2], Mercedes M. Pascual[3,4], Donald C. Keenan[5], Andrew N. Dobson[4,6] and Matthew H. Bonds[7,8,9]

[1]Department of Mathematics, University of Florida, Gainesville, FL, 32611, USA. [2]Department of Biology, Hopkins Marine Station, Woods Institute for the Environment, Center for Innovation in Global Health, Stanford University, Pacific Grove, CA, 93950, USA. [3]Department of Ecology and Evolution, University of Chicago, Chicago, IL, 60637, USA. [4]Santa Fe Institute, Hyde Park Road, Santa Fe, NM, 87501, USA. [5]Université de Cergy-Pontoise et THEMA, Cergy-Pontoise Cedex, 95011, France. [6]Department of Ecology and Evolutionary Biology, Princeton University, Princeton, NJ, 08544, USA. [7]Department of Global Health and Social Medicine, Harvard Medical School, Boston, MA, 02115, USA. [8]PIVOT, Boston, MA, 02115, USA. [9]Stanford School of Medicine, Palo Alto, CA, USA. *e-mail: calistusnn@ufl.edu

General ecological models for human subsistence, health and poverty

Calistus N. Ngonghala[1,*], Giulio A. De Leo[2], Mercedes M. Pascual[3,6], Donald C. Keenan[4], Andrew N. Dobson[5,6] & Matthew H. Bonds[7]

[1]*Department of Mathematics, University of Florida, Gainesville, FL 32611*

[2]*Department of Biology, Hopkins Marine Station, Woods Institute for the Environment, Center for Innovation in Global Health, Stanford University, Pacific Grove, CA 93950*

[3]*Department of Ecology and Evolution, University of Chicago, Chicago, IL 60637*

[4]*Université de Cergy-Pontoise et THEMA, 95011 Cergy-Pontoise, Cedex, France*

[5]*Department of Ecology and Evolutionary Biology, Princeton University, Princeton, NJ 08544*

[6]*Santa Fe Institute, Hyde Park Road, Santa Fe, NM 87501*

[7]*Department of Global Health and Social Medicine Harvard Medical School, Boston, MA 02115*

Online Supplementary information

S1 Model development

As general background for the construction of the coupled ecological-economic-natural enemy models, we present a brief overview of well-known and basic classical models in population ecology and infectious diseases of humans (Section S1.1.1), renewable resources (Section S1.1.2), agricultural pests (Section 1.1.3), and economic growth theory (Section S1.1.4). These models are coupled together in various ways in Section S1.2. Dynamical properties and bifurcation diagrams illustrating the dynamics of some of the systems are presented in Sections S3.2-S3.3, while sensitivity analyses results are presented in Section S4.

S1.1 Basic elements of the coupled models

S1.1.1 Population biology and infectious disease models

Classical models in population biology assume the general form:

$$\dot{x} = \psi(x) - \delta(x)x,$$

where ψ and δ are the population growth (e.g., birth and immigration) and loss (e.g., mortality and emigration) rates. The simplest case is when $\psi(x) = \lambda x$ and $\delta(x) = \mu$, where $\lambda > 0$ and $\mu > 0$ are constants so that the population experiences exponential growth (decay), when $\lambda > \mu$ ($\lambda < \mu$). However, for biological realism, density dependence is introduced in the growth or loss rate or in both. Typical functional forms to represent density dependence include logistic growth and Holling-type I, II and III functional responses (for linear, saturating and sigmoidal variation with density, respectively). More mechanistic representations of the limits to growth consider "natural enemies" in the form of predators, competitors, pathogens, etc. These systems require at least two equations–one for the population and the other for the enemy[1].

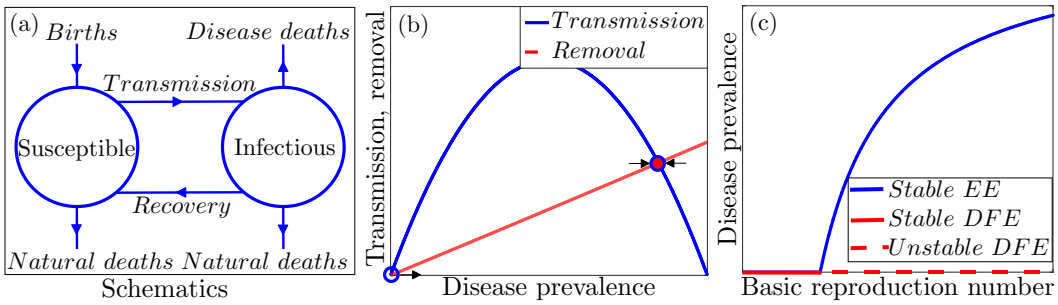

Figure S1: **Schematics and dynamics of simple disease model**. (a) Transitions between the susceptible (healthy) and infectious (unhealthy) compartments. Individuals are born susceptible and die at a natural rate, while infectious individuals may die naturally or from infection. (b) Equilibria occur where disease transmission intersects removal (recovery and mortalities) from infection. A maximum of two equilibria, a disease-free equilibrium (open circle) and an endemic equilibrium (closed circle), is possible. (c) Bifurcation diagram showing a globally stable disease-free equilibrium (DFE: solid red line) when the basic reproduction number is less than one, and a globally stable endemic equilibrium (EE: solid blue line) when the basic reproduction number is greater than one.

While there is a variety of potential natural enemies of humans, here we focus on infectious diseases because of their pervasiveness, especially in populations afflicted by poverty. As a broad ecological class, infectious diseases are the most important cause of morbidity and mortality of most biological species, including humans throughout history and of the poor today. Models of infectious disease dynamics are typically based on a classical compartmentalized formulation[2–6], the most basic of which consists of two states: susceptible (uninfected and non-immune individuals), denoted by $\tilde{S}$, and infectious (those infected and who can transmit the disease), denoted by $\tilde{I}$, with the total population size given by $N = \tilde{S} + \tilde{I}$. This model and the many variants, which include other states such as "exposed" and "recovered" have been useful in providing insights into the dynamics of many diseases of humans, animals and plants. For simplicity, we focus on susceptible-infectious-susceptible (SIS) models (schematics and sample dynamics in Fig. S1 (a)-(b)), which have been applied to many kinds of bacterial and helminth infections, including diarrheal pathogens and sexually transmitted diseases that do not trigger permanent immune response. The model is governed by the system of first order ordinary differential equations:

$$\dot{\tilde{S}} = \lambda N + \gamma \tilde{I} - \frac{\beta \tilde{I}}{N}\tilde{S} - \mu \tilde{S}, \tag{S1}$$

$$\dot{\tilde{I}} = \frac{\beta \tilde{I}}{N}\tilde{S} - (\gamma + \mu + \nu)\tilde{I}. \tag{S2}$$

where λ is the birth rate, β is the transmission rate, γ is the recovery rate, μ is the natural mortality rate, ν is the disease-imposed mortality rate. Because $N = \tilde{S} + \tilde{I}$, if we set $\tilde{S} = N - \tilde{I}$, then Equations (S1)-(S2) reduce to the single equation:

$$\dot{\tilde{I}} = \frac{\beta \tilde{I}}{N}(N - \tilde{I}) - (\gamma + \mu + \nu)\tilde{I}, \tag{S3}$$

which assumes the form of the general equation for the natural enemy (Equation (2)) in the main text. Setting $I = \tilde{I}/N$, where I is the proportion of infectives, Equation (S3) becomes:

$$\dot{I} = \beta(1 - I)I - (\gamma + \nu + \lambda)I + \nu I^2. \tag{S4}$$

Equation (S4), has one stable infection-free equilibrium (DFE: solid red line in Fig. S1 (c)), $I^0 = 0$, when $0 < R_0 < 1$, and one globally stable endemic equilibrium (EE: solid blue line in Fig. S1 (c))

$I^* = \frac{(\gamma+\nu+\lambda)(R_0-1)}{\beta-\nu}$, when $R_0 > 1$. The basic reproduction number, $R_0 = \frac{\beta}{\gamma+\nu+\lambda}$, represents the average number of new infections in a susceptible population, which are attributable to one infectious individual over its whole infectious period[7,8].

S1.1.2 Renewable resource model

Plant density, agriculture, or renewable resource is modeled through the plant-grazing framework of Noy-Meir[9] or the plant growth frameworks in van de Koppel et al.[10] and Rietkerk and van de Koppel[11]. These models explore the impact of limiting factors such as water availability on plant growth. In their basic forms, these models and others use the classical logistic growth function[12] with adjustments to account for harvesting and processes that reduce plant density such as grazing by herbivores. The general framework is:

$$\dot{c} = \psi(c) - \delta(c)c, \tag{S5}$$

where c is the the plant standing of crop, ψ is the plant growth term and δ is the plant loss term. In addition to the logistic functional form, ψ can be modeled through other nonlinear functional forms[13], while the loss rate function δ can be modeled using various Holing-type functional responses or other nonlinear forms. In Noy-Meir[9], ψ is modeled using the logistic functional form $r_c c(1 - c/C_0)$, where r_c is the intrinsic growth rate of the plants and C_0 is the carrying capacity, while in van de Koppel et al.[10], ψ is modeled with the equation $\psi(c) = r_c c(1 - c/C_0)\zeta(W)$, where the function, $\zeta(W)$ captures the effect of plant growth limiting factors such as water or salt level on plant growth. We adopt the same kind of framework here, with c representing renewable resource density and r_c the renewable resource intrinsic growth rate. These renewable resource equations can be adapted, with slight modifications to other coupled agricultural processes including livestock and fishery. They can also be extended to incorporate economic growth theory, if the limiting factor of plant growth or the renewable resource is viewed as capital, which, of course, provides one way of coupling the renewable resource and economic growth models.

S1.1.3 Agriculture-pest model

This model is based on the classical predator-prey framework[14] with the pest p, serving as the predator and the crop c, the prey. The framework in Hillier and Birch[15] is:

$$\dot{c} = r_c c(1 - c/c_0) - bcp, \tag{S6}$$

$$\dot{p} = \omega bcp - dp, \tag{S7}$$

where r_c is the intrinsic agricultural product growth rate, c_0 is carrying capacity, b is a measure of the rate at which the agricultural product is consumed by the pest, $0 \leq \omega < 1$ is the conversion factor from crop biomass to pest biomass, and d is the pest mortality rate. This model can easily be extended to account for multiple pest species (see Hillier and Birch[15]). We briefly recall the dynamics of Equations (S6)-(S7) (see references[15,16] for details). The model exhibits a trivial equilibrium $E_0^* = (0, 0)$ and two additional equilibria–$E_c^* = (c_0, 0)$ and $E_{cp}^* = (d/(br_c), 1 - d/(c_0 br_c))$. The equilibrium point E_0^* is unstable, E_c^* is stable when $d/(c_0 br_c) > 1$, and E_{cp}^* is globally stable when $d/(c_0 br_c) < 1$. Stability of E_{cp}^* implies co-persistence of the crop and pest. As with the infectious disease and renewable resource models (Equations (S4) and (S4), respectively), the crop-pest model (Equations (S6)-(S7)) can have only one stable equilibrium.

S1.1.4 Economic growth model

In the economics literature, income generation is often modeled from "production functions", where $Y = Y(\mathbf{X}, L)$, is output or income, L is labor, and $\mathbf{X}$ is a vector of different forms of capital. The standard neoclassical economic growth model[17] originally focused on physical capital (e.g., infrastructure and equipment), but other subtler forms of capital, such as human capital (education or health), have become routinely incorporated into models of economic growth. As for biological populations, economic growth can be modeled as a dynamical system (schematics in Fig. S2 (a)), where capital is a state variable:

$$\dot{X}_i = r_i Y(\mathbf{X}) - \delta_i X_i, i = 1, 2, 3, \ldots, M.$$

The subscript i refers to a specific form of capital, r is the rate of capital accumulation (i.e., savings), and δ is the rate of capital depreciation (schematics are presented in Fig. 1(a)). Economic growth is thus generated from a system of reinforcing feedbacks, where income that is not consumed is reinvested into capital. A simple example of a production function is the Cobb-Douglas[18]:

$$Y(\mathbf{X}, L) = A \prod_{i=1}^{M} X_i^{\alpha_i} L^{1-(\sum_{i=1}^{M} \alpha_i)},$$

where A is a productivity term (technological progress, total production factor, or labor efficiency), and α is the production elasticity (the percent change in output that results from a percent change in capital). A common assumption is that the inputs exhibit decreasing returns to scale, such that $\sum_i \alpha_i < 1$[19]. We can express A, as $A = \phi \Phi^{1-(\sum_{i=1}^{M} \alpha_i)}$, where ϕ is a positive constant and $\Phi^{1-(\sum_{i=1}^{M} \alpha_i)}$ is some labor coefficient or labor efficiency. Per capita units can be calculated by dividing income and the various forms of capital by labor, L, i.e., $y = Y/L$ and $x_i = X_i/L$, which yields $y = A \prod_{i=1}^{M} x_i^{\alpha_i}$, where $A = \phi \Phi^{1-(\sum_{i=1}^{M} \alpha_i)}$, and

$$\dot{x}_i = r_i y - (\delta_i + n) x_i. \tag{S8}$$

The x_i's thus represent different forms of capital per "effective units of labor", y represents income per effective units of labor and n is the rate of per capita population growth.

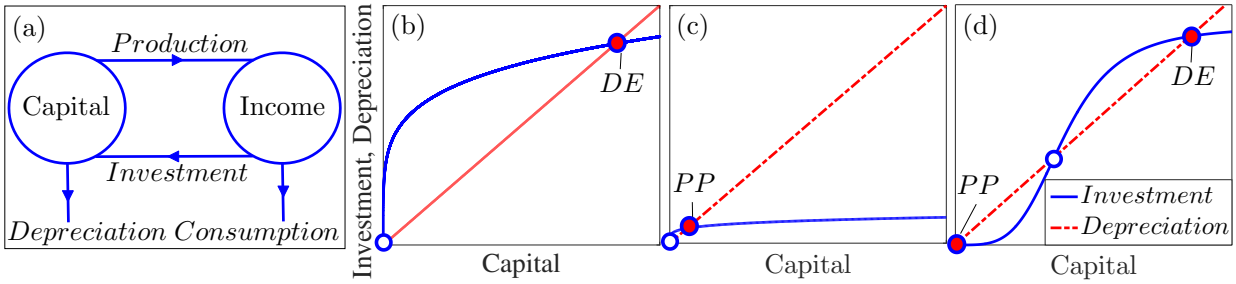

Figure S2: The neoclassical growth model: $\dot{X} = rY(X) - \delta X$. (a) Schematics. Through the production process, capital generates income. A portion of the income is consumed, while the other portion is reinvested into capital. Capital is lost through depreciation. (b)-(d) The y-axis represents the rate of change in capital, and the x-axis depicts the stock of capital. The growth rate of the economy depends on the investment, $rY(X)$ (blue line) relative to depreciation δX (red line). Equilibria are given by the intersection between the investment and depreciation curves. When investment is above depreciation, capital accumulates and the economy grows. When investment falls below depreciation, capital is lost and the economy shrinks. The traditional model depicted in (b)-(c) has one unstable equilibrium (open circle) at the origin and one stable equilibrium, and thus the system is globally stable. (c) Persistent poverty can be caused by a low savings rate, r. (d) Poverty trap caused by a nonlinear capital accumulation curve, such that the rate of investment is lower than the rate of depreciation in part of the state space. An unstable equilibrium is sandwiched between two stable equilibria, depicting bistability[20].

Models of economic growth can allow us to explore concepts of economic stagnation, such as "poverty traps", defined as self-reinforcing systems that cause poverty to persist[20–22]. Using this framework, a poverty trap is characterized as an equilibrium level of income that is low and stable. Figure S2 (b)-(c) depicts the simplest conceptualization of a poverty trap using the neoclassical growth model, where the difference between the two stable equilibria, denoted by filled circles, is determined by different parameters: the development equilibrium, DE (Fig. S2 (b)), results from a high savings rate, r, and the persistent poverty, PP (Fig. S2 (c)), results from a low savings rate. In either case (Fig. S2 (b)-(c)), the stability is global and therefore all initial conditions result in the same final outcome. In contrast, the more canonical depiction of a poverty trap is characterized by multiple locally stable equilibria, such that the outcome is dependent on initial conditions of the state variables and a market or environmental shock can push the system from the basin of attraction of one locally stable equilibrium to the other (Fig. S2 (d)). This can result, for example, when the rate of savings is itself a nonlinear function of capital, $r = r(x)$, or from nonlinear capital accumulation curves (Fig. S2 (d)). Populations with initial levels of capital that are less than the threshold

level (the unstable equilibrium denoted by the open circle) are in the basin of attraction of the poverty trap (investment $<$ depreciation), while capital levels that are greater than the threshold level, fall in the basin of attraction of the good (or rich) equilibrium (investment $>$ depreciation)[20,23]. Important questions for an ecological framework relate to how biological processes influence capital accumulation.

S1.2 Specific coupled models formulated under the general framework in the main text

The general framework for coupled ecological-economic systems is presented in the body of the main paper (Equations (1)-(2)). In this section, we present a series of specific models, including those in the main text, that combine the dynamics of capital with those of disease and renewable resources. We first present systems (i)-(vi) in Table 2 of the main paper, and include a further set of variations (including systems (vii)-$(viii)$ in Table 2 and the additional systems listed in Table S1) on these initial models that allow for further complexity, including explicit demography. Tables 2 and S1 summarize the specific components of each of the models. Consideration of a broad range of models allow us to address the generality of the results, especially those on the sensitivity analyses (Section S4).

S1.2.1 Models (i)-(iii) in the main text: coupled disease-economic growth models

Infectious disease models can be coupled to economic growth models through two underlying principles for which there is overwhelming empirical evidence: 1) income influences the transmission and recovery rates of diseases; and 2) disease influences income through human capital and population growth. Although different functional forms can be employed to reflect how income may affect disease dynamics, here, we present one general class of functions for the transmission rate β, and the recovery rate γ, that can give rise

to a wide range of specific relationships depending on the specific parameters:

$$\beta(y) = \frac{\beta_{max}\beta_y^\kappa}{y(t)^\kappa + \beta_y^\kappa}, \tag{S9}$$

$$\gamma(y) = \frac{\gamma_{min}\gamma_y(y(t)^\kappa + y_0)}{y_0'(y(t)^\kappa + \gamma_y)}, \tag{S10}$$

where $\kappa > 0$ is a constant that determines the shape of β and γ (linear, concave or sigmoidal), $\beta_{max} > 0, \beta_y > 0, \gamma_{min} > 0, \gamma_0' > 0$, and $\gamma_y > y_0 > 0$ are exogenous parameters, with β_{max} and γ_{min} representing maximum transmission and minimum recovery rates respectively, and β_y is the amount of income necessary to attain half the disease transmission rate. Though the specific shape of these functions depends on the parameters, they broadly imply that as income rises, the transmission rate falls and the recovery rate rises (as a result of better access to preventive care, sanitation, clean water, better hygiene, nutrition, education, etc.), which corresponds to the assertion that poverty is an underlying cause of disease[24,25].

The mechanism through which disease influences economic growth can be through the accumulation of human capital:

$$r(I) = r_h\Phi(I), \;\; \Phi(I) = (1 - \xi I)^m, \tag{S11}$$

where the parameter r_h can be considered the rate of spending on education or other activities for child development, which converts to human capital at a rate that depends on the health of the child. This structure is based on substantial evidence that diseases can cause significant decreases in school performance and attendance, even for infections, such as helminth infections, that have little outward signs of morbidity[26,27]. Equation (S11) indicates that the maximum accumulation of human capital, r, occurs when the disease burden, I, is 0. Conversely, the rate of human capital accumulation approaches 0 as the disease burden approaches 1. The parameters m and ξ determine the curvature presented in Fig. 1. Disease burdens can be measured in variety ways, including in particular disability adjusted life years (DALYs) and disease prevalence. If we assume here, for heuristic purposes, that all infections have an equal effect on reducing human capital accumulation (e.g., through school absence), then m (Equation (S11)) can be interpreted as the number of different pathogens in the system. Host-parasite models that examine the dynamics of multiple

pathogens have increasingly complex transient dynamics; for simplicity, we maintain the host population at a constant density and assume no immunological or competitive interactions between the pathogens. On the other hand, $0 \leq \xi \leq 1$ represents the severity of the pathogens on the ability to invest. For example, if $\xi = 0$, the diseases have no impact on the process of human capital accumulation.

Disease can also influence economic growth by reducing labor productivity and hence income directly, e.g., when sick people cannot work– in which case per capita income is:

$$y(\mathbf{x}, I) = \phi f(\mathbf{x}, I) = \phi \Phi(I)^{\left(1-\sum_{i=1}^{M} \alpha_i\right)} \prod_{i=1}^{M} x_i^{\alpha_i}, i = 1, 2, 3, \ldots, l, \tag{S12}$$

where $f(\mathbf{x}, I) = \Phi(I)^{\left(1-\sum_{i=1}^{M} \alpha_i\right)} \prod_{i=1}^{M} x_i^{\alpha_i}$. Here, $A(I) = \phi \Phi(I)^{\left(1-\sum_{i=1}^{M} \alpha_i\right)}$, and $\Phi(I) = (1 - \xi I)^m$. Figure S3 shows one way of coupling models that are rooted in population ecology and economic growth.

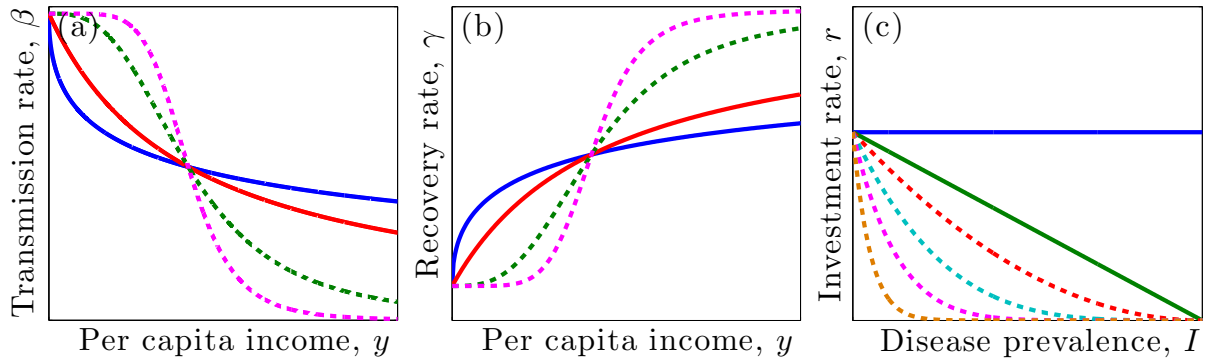

Figure S3: (a)-(b) Functional relationships between the transmission rate β, the recovery rate γ, and per capita income y. The nonlinearity and thus the possibility of multiple equilibria increases with the shape constant k, from the solid blue curve to the dashed magenta curve. (c) Functional relationship between the rate of investment in human capital h, and disease prevalence I. The relationship is constant when there is no pathogen (solid blue line), i.e., $r = r_h$; linear and monotonic decreasing in the presence of one pathogen (solid green line), i.e., $r = r_h(1 - \xi I)$ and nonlinear, with the nonlinearity increasing with the number of pathogens in the presence of more than one pathogen (dashed curves), i.e., $r = r_h(1 - \xi I)^m, m > 1$.

With β, γ, and r as defined in Equations (S9)-(S11), we recover the type of basic coupled model presented in Ngonghala et al.[23], by setting $\xi = 1$, which corresponds to cases where children stop attending school for the duration of infection, $y = f(0, h, 0) = \phi \Phi(0) h^{\alpha_h} = \phi h^{\alpha_h}$, $n = 0$, i.e., the population size

is constant (the disease is non-fatal, and births and deaths are equal), $\kappa = 1$, and by assuming that there is only one form of capital (human capital, h). The system is:

$$\dot{h} = r_h(I)y - \delta_h h, \tag{S13}$$

$$\dot{I} = \beta(y)(1-I)I - \gamma(y)I, \tag{S14}$$

This basic model corresponds to Model (i) described in Table 2 of the main text. The difference between this model and that in Ngonghala et al.[23] is in the production function (Cobb-Douglas[18] here as opposed to constant elasticity of substitution[17,28] in Ngonghala et al.[23]). Since the dynamics of many infectious diseases occur on shorter time scales than economic dynamics, which can occur over the course of generations, we assume that infectious disease dynamics quickly reach a quasi-steady state. Thus, solving for a "quasi-steady state" in disease (i.e., where $\dot{I} = 0$), we can reduce Equations (S13)-(S14) to:

$$\dot{h} = r_h(\gamma/\beta)^m y - \delta_h h. \tag{S15}$$

Model (ii) is obtained from model (i) by incorporating disease explicitly in the income equation ($y = f(0,h,I) = \phi\Phi(I)h^{\alpha_h}, \Phi(I) = (1-\xi I)^m, I \neq 0$), representing lost labor productivity. In deriving models (i) and (ii), we assumed that there is only one form of capital (human capital). But if there is another form of capital (physical capital, k) and disease decreases labor productivity as in model (ii), then the income function must be modified accordingly: $y = \phi f(k,h,I)$, where $f(k,h,I) = \Phi(I)^{(1-\alpha_h-\alpha_k)}h^{\alpha_h}k^{\alpha_k}$. The resulting system corresponds to Model (iii) in Table 2 of the main text:

$$\dot{k} = r_k y - \delta_k k, \tag{S16}$$

$$\dot{h} = r(I)y - \delta_h h, \tag{S17}$$

$$\dot{I} = \beta(y)I(1-I) - \gamma(y)I. \tag{S18}$$

S1.2.2 Models (iv)-(vi) in Table 2 of the main text: coupled economic-renewable resource model

Both human capital in the form of knowledge, skills, education, health, etc., and physical capital in the form of machinery, infrastructure, other agricultural equipment, etc., are required to boost agricultural productivity and harvesting effort. For example, motorization allows fishermen to access offshore fishery that otherwise might not be accessible, mechanization of agriculture allows for the cultivation of wider fields and the use of fertilizers to boost productivity. Hence, the renewable resource model defined by Equation (S5) can be coupled to the economic growth model by assuming that the production of the resource is limited by the availability of capital. This can be achieved by setting the carrying capacity to: c_0E, where $c_0 > 0$ is a constant, and $E = k^{\alpha_k}h^{\alpha_h}$. Additionally, the renewable resource model is coupled to the economic model through the harvesting effort $\delta_c E$, which we also assume is a function of capital, since harvesting requires economic resources. Here, $\delta_c > 0$ is the harvest rate. On the other hand, we couple the economic model back to the renewable resource model through investment in capital. If μ_c is the grazing or loss rate of renewable resources, then the coupled economic growth-renewable resource model is given by the system:

$$\dot{k} = r_k y - \delta k, \tag{S19}$$

$$\dot{h} = r_h(0) y - \delta h, \tag{S20}$$

$$\dot{c} = r_c c\left(1 - \frac{c}{c_0 E}\right) - (\delta_c E + \mu_c)c, \tag{S21}$$

where $y = (\phi + \pi_c\delta_c c)f(k,h,0), E = f(k,h,0)$, and $f(k,h,0) = \Phi(0)^{(1-\alpha_k-\alpha_h)}k^{\alpha_k}h^{\alpha_h} = k^{\alpha_k}h^{\alpha_h}$. Here, $\pi_c\delta_c c k^{\alpha_k}h^{\alpha_h}$ is the income derived from the exploitation of renewable resources, $\phi k^{\alpha_k}h^{\alpha_h}$ is the income from other sources and π_c is the unit cost of renewable resources. Equations (S19)-(S21) is Model (iv) in Table 2 in the main text.

Introducing the dynamics of human disease (by adding Equation (S14) to Equations (S19)-(S21)) and setting $I \neq 0$ in the human capital and income equations in Model (iv) (Equations (S19)-(S21)) so that $y = (\phi + \pi_c\delta_c c)f(k,h,I)$, where $f(k,h,I) = \Phi(I)^{(1-\alpha_k-\alpha_h)}k^{\alpha_k}h^{\alpha_h}$ leads to Model (v) in Table 2 of the

manuscript. Next, we extend Model (v) – the coupled economic growth-renewable resource-human disease model to account for the dynamics of agricultural pest. This leads to Model (vi) in Table 2:

$$\dot{k} = r_k y - \delta_k k, \tag{S22}$$

$$\dot{h} = r_h(I) y - \delta_h h, \tag{S23}$$

$$\dot{c} = r_c c \left(1 - \frac{c}{c_0 E}\right) - (b(y)p + \delta_c E + \mu_c)c, \tag{S24}$$

$$\dot{p} = \omega b(y) c p - d(y) p, \tag{S25}$$

$$\dot{I} = \beta(y) I(1 - I) - \gamma(y) I, \tag{S26}$$

where y is as described in Model (v), $b(y) = b_{max} b_y/(y + b_y), d(y) = d_{min} d_y(y + 1))/(y + d_y)$, b_y and d_y are positive constants, b_{max} is the maximum consumption rate of agricultural products by pest, and d_{min} is the minimum mortality rate of pests. Since, the poor rely mostly on their immediate environment for subsistence, we assume for simplicity that income from other sources is small compared to income from renewable resources. Decreasing returns to capital ensure that plant density and the yield do not grow indefinitely with capital. The renewable resource equation takes the form of the economic capital equation, with an investment or gain term and a loss term. Here, income is a function of disease prevalence, human capital, physical capital, and renewable resource density. A poverty trap corresponds to high disease prevalence, low per capita income and renewable resource density, while the development equilibrium corresponds to low disease prevalence and high per capita income, as well as high renewable resource density.

S1.2.3 Additional models

Based on the set of economic, renewable resource and disease model elements presented in Table 1 in the main text and described in Section S1.1, we can generate additional variants of of the coupled systems with different levels of complexities. Some of these extensions are presented in Table 2 of the main text and Table S1 below. Specifically, a variant of Model (iv) leads to a system with agricultural pest but no human disease (Model iv' in Table S1). The next set of models ((vii)-$(viii)$ in Table 2 of the main text) and models ((ix)-

(x) in Table S1) incorporates demographic changes: human births, natural mortality and disease-induced mortality in models (iii) and (v) and models (ii) and (vi), respectively. The birth and natural mortality rates can assume various functional forms (constants, density-dependent functions, functions of income or capital, etc.)

Table S1: **Additional models.** System (iv') has both human capital $((h))$ and physical capital $((k))$, renewable resource $((c))$ and plant pest $((p))$ but no human disease $((I))$ and no human population growth $((n))$. Model (ix) has only one form of capital (human capital), human disease, and human population growth, while Model (x) incorporates human disease and human population growth in Model (iv'). Here, $f(k,h,I) = \Phi(I)^{1-\alpha_k-\alpha_h} k^{\alpha_k} h^{\alpha_h}$, λ is the human birth rate, μ and ν are the human natural and disease mortality rates, and $n = \lambda - \mu - \mu I$.

Model	h	$h(I)$	k	$y(I)$	c	p	n	Income function and model equations
(iv')	✓		✓		✓	✓		$y_4 = (\phi + \pi_c \delta_c c) f(k,h,0), \quad E = k^{\alpha_k} h^{\alpha_h},$ $\dot{k} = r_k y_4 - \delta_k k,$ $\dot{h} = r_h y_4 - \delta_h h,$ $\dot{c} = r_c c\,(1 - c/(c_0 E)) - (\delta_c E + \mu_c) c.$ $\dot{p} = \omega b(y_4) pc - d(y_4) p.$
(ix)	✓	✓		✓			✓	$y_2 = \phi f(0,h,I),$ $\dot{h} = r_h \Phi(I) y_2 - (\delta_h + n(I)) h,$ $\dot{I} = \beta(y_2)(1-I)I - (\gamma(y_2) + \nu + \lambda) I + \nu I^2.$
(x)	✓	✓	✓	✓	✓	✓	✓	$y_5 = (\phi + \pi_c \delta_c c) f(k,h,I), \quad E = k^{\alpha_k} h^{\alpha_h},$ $\dot{k} = r_k y_5 - (\delta_k + n(I)) k,$ $\dot{h} = r_h \Phi(I) y_5 - (\delta_h + n(I)) h,$ $\dot{c} = r_c c\,(1 - c/(E)) - (\delta_c E + \mu_c) c,$ $\dot{I} = \beta(y_5)(1-I)I - (\gamma(y_5) + \nu + \lambda) I + \nu I^2.$ $\dot{p} = \omega b(y_5) pc - d(y_5) p.$

S2 Model parameterization

S2.1 Calibration of the basic disease-economic model (i) (Equations (S13)-(S14)

We apply the maximum likelihood estimator (MLE) approach[29,30] to calibrate the parameters, $\theta = (\beta_{max}, \beta_y, \gamma_{min}, \gamma_y, m, r_h, \delta_h, \alpha_h)$ by fitting the basic coupled disease-economic model $((i))$ to data on per capita income (per capita GDP) and the burden of infectious diseases (DALYs)[31–33]. Per capita GDP and DALY are the most common annualized measurements of economic production (i.e., per capita income) and disease burden, respectively. We treat m as a free parameter to represent the "effective" number of diseases, given

that there are many different kinds of infections that are aggregated in the data (such as diarrheal diseases and respiratory infections), each with different parameter values and population dynamics. Here, we use the log of the likelihood function:

$$\ln \mathcal{L}(x|\theta) \quad = \quad \ln \left(\prod_{j=1}^{N} \frac{1}{\sqrt{2\pi\sigma^2}} e^{-\frac{(x_j - z_j)^2}{2\sigma^2}} \right) = -\frac{1}{2} \left(N \ln(2\pi) + N \ln(\sigma^2) + \sum_{j=1}^{N} \frac{(x_j - z_j)^2}{\sigma^2} \right),$$

where $x = (DALY, GDP)^T, z(\theta) = (I(\theta), y(\theta))^T$. The MATLAB nonlinear constrained optimization function, "$fmincon$" is used to maximize this function and obtain the estimate $\beta_{max} = 17, \beta_y = 34, \gamma_{min} = 9, \gamma_y = 40, m = 3, r_h = 0.3$, and $\delta_h = 0.27, \alpha_h = 0.6$.

The model calibration presented here is meant to be a simple illustration of how the models we develop can be parameterized, if data is available. Different approaches including Bayesian approaches can be used with the availability of appropriate data. For the demographic parameters, we assume that the birth rate ranges from 7-46 births per thousand per year and that the average life span of humans ranges from 40-80 years[34,35]. With these ranges, we obtain an average birth and death rate of 0.027 (about 37 births per thousand per year) and 0.019 (an average life span of about 53 years). For the accumulation and depreciation rates of physical capital, we also use the calibrated values for human capital and for the elasticity coefficients, we draw values from the economics literature, e.g., $\alpha_h = \alpha_k \approx 0.3$ as in Mankiw et al.[19]. The models in Table 2 of the main text and Table S1 integrate classical ecological and economic models. These coupled systems are different from classical ecological or economic models, such that most of the parameters are functions of other state variables, e.g., capital, disease prevalence, biomass of the renewable resource, or a combination of these–as well as new parameters that have not been explored in the literature. This makes obtaining parameter values, especially those for the more complex systems, challenging and highlights the need for future empirical research to collect data so that key parameters can be estimated. For the parameters whose values we cannot find in the literature, such as for the renewable resources and pests, we estimate them such that at the development or poverty trap equilibrium, income and disease prevalence are

within observed ranges. For example, income ranges from approximately \$300-\$50,000. We note that these specific values are used only for selected simulations and bifurcation analyses. The parameter values and ranges of parameters used in our analyses are presented in Table S2. For more general analyses, we use Latin Hypercube Sampling to conduct global sensitivity analyses (described later on in Section S4 of the SI) that explore ranges of parameters. See Table S2 for a brief description of model parameters, baseline values and ranges. For parameters whose ranges are not between zero and one or parameters whose ranges we could not find or infer directly from the literature, we define the ranges to have a minimum and maximum of $\pm 50\%$ of the baseline value, while ensuring that the minimum and maximum values are ecologically and economically feasible.

In the absence of appropriate data for implementing actual inference efforts as is the case here, we can also parameterize the system by selecting reasonable model parameters and ranges and investigating the plausible dynamics in a more theoretical approach. Specifically, parameters (and ranges) can be selected that lead to a poverty equilibrium approximately equivalent to the average per capita income in developing countries (below 2 US dollars per day used as a threshold for poverty), and to a development equilibrium approximately equivalent to average per capita income in developed countries (see, for example, Table S3). Therefore, we can define plausible ranges of variation of model parameters that lead to prevalence and income values within the range of variation observed in empirical studies. We thus believe that our models are able to capture the fundamental processes driving the reinforcing feedback between poverty and diseases and, in a significant number of cases, leading to bistability where the final outcome is contingent on history. We believe that one important outcome of formulating the models, is to stimulate the needed work to better parameterize specific systems that fall within this general framework.

Table S2: Brief description of parameters, baseline values and sample ranges for the models in Tables 2 of the main text and Table S1.

Parameter	Description	Value	Range
Human disease			
β_{max}	Maximum human disease transmission rate	17	[8.5, 25.5]
β_y	Positive constant	34	[17, 51]
γ_{min}	Minimum human recovery rate	9	[4.5, 13.5]
γ_y	Positive constant	40	[20, 60]
m	Number of pathogens	3	[0, 8]
ξ	Disease intensity	0.6	[0, 1]
ν	Disease-induced mortality	0.1	[0.05, 0.15]
Economic			
$r_h,\ r_k$	Human and physical capital accumulation rates	0.3	[0.15, 0.45]
$\delta_h,\ \delta_k$	Human and physical capital depreciation rates	0.27	[0.1, 0.4]
α_h, α_k	Elasticity coefficient	0.3, 0.6	[0.15, 0.45], [0.3, 0.9]
ϕ	Technology	0.4, 1	[0, 1]
π_c	Unit cost of harvested resource	2	[1, 4]
Renewable resource			
r_c	intrinsic growth rate of renewable resource	0.2, 0.8	[0.1, 0.4], [0.4, 1.2]
δ_c	Resource harvest constant	0.1	[0.05, 0.2]
c_0	Scaling factor of resource carrying capacity	10	[5, 20]
μ_c	Grazing or additional loss rate of renewable resource	0.02	[0.01, 0.04]
Plant pest			
ω	Coefficient of conversion from renewable resource biomass and pest abundance	0.8	[0.4, 1.2]
b_{max}	Maximum plant disease transmission rate	1	[0.5, 1.5]
b_y	Positive constant	2	[1, 3]
d_{min}	Minimum pest mortality rate	1	[0.5, 1.5]
d_y	Positive constant	5	[2.5, 7.5]
Human demography			
λ_{max}	Maximum human birth rate	0.05	[0.025, 0.075]
λ_{min}	Minimum human birth rate	0.01	[0.005, 0.015]
μ_{max}	Maximum human mortality rate	0.025	[0.0125, 0.0375]
μ_{min}	Minimum human mortality rate	0.0133	[0.01, 0.02]
τ_λ	Decay constant human birth rate	0.95	[0.5, 1]
τ_μ	Decay constant for human mortality rate	0.05	[0, 0.5]

Table S3: Brief description of parameters and alternative parameterization of the models in Tables 2 of the main text and Table S1. This approach entails selecting parameters and ranges such that the poverty equilibrium ia approximately equivalent to average per capita income in developing countries, while the development equilibrium is approximately equivalent to average income in developed countries.

Parameter	Description	Value	Range
Human disease			
β_{max}	Maximum human disease transmission rate	5	[2.5, 7.5]
β_y	Positive constant	4.5	[2.25, 6.75]
γ_{min}	Minimum human recovery rate	2	[1, 3]
γ_y	Positive constant	0.9	[0.45, 1.35]
m	Number of pathogens	4	[0, 8]
ξ	Disease intensity	0.6	[0, 1]
ν	Disease-induced mortality	0.1	[0.05, 0.15]
Economic			
$r_h,\ r_k$	Human and physical capital accumulation rates	0.2	[0.1, 0.3]
$\delta_h,\ \delta_k$	Human and physical capital depreciation rates	0.1	[0.05, 0.15]
α_h, α_k	Elasticity coefficient	0.3, 0.5	[0.15, 0.45], [0.25, 0.75]
ϕ	Technology	0.4, 2, 3	[0.2, 0.6], [1, 3], [1.5, 4.5]
π_c	Unit cost of harvested resource	1	[0.5, 1.5]
Renewable resource			
r_c	intrinsic growth rate of renewable resource	0.2, 0.8	[0.1, 0.4], [0.4, 1.2]
δ_c	Resource harvest constant	0.1	[0.05, 0.2]
c_0	Scaling factor of resource carrying capacity	1	[0.5, 1.5]
μ_c	Grazing or additional loss rate of renewable resource	0.02	[0.01, 0.04]
Plant pest			
ω	Coefficient of conversion from renewable resource biomass and pest abundance	0.8	[0.4, 1.2]
b_{max}	Maximum plant disease transmission rate	0.03	[0.015, 0.045]
b_y	Positive constant	1	[0.5, 1.5]
d_{min}	Minimum pest mortality rate	0.01	[0.005, 0.015]
d_y	Positive constant	0.02	[0.01, 0.03]
Human demography			
λ_{max}	Maximum human birth rate	0.05	[0.025, 0.075]
λ_{min}	Minimum human birth rate	0.01	[0.005, 0.015]
μ_{max}	Maximum human mortality rate	0.025	[0.0125, 0.0375]
μ_{min}	Minimum human mortality rate	0.0133	[0.01, 0.02]
τ_λ	Decay constant human birth rate	0.95	[0.5, 1]
τ_μ	Decay constant for human mortality rate	0.05	[0, 0.5]

S3 Dynamics and analyses of model systems

We begin with some general analytical considerations on the types of dynamics the coupled systems presented in Tables 2 and S1 and explained in Section S1 can exhibit. Because these considerations are limited to the simplest formulations, we then follow with specific analyses based on bifurcation diagrams which complement those in the main text. We then transition to the broader investigation of parameter space including sensitivity analyses.

S3.1 Dynamical properties of the systems

The dynamics of systems (i)-(iii) and (vii) in Table 2 of the main text, as well as those of model (ix) in Table S1 are characterized by fundamental mechanisms of positive feedback. Therefore, bistability is potentially a general property of these systems. This behavior contrasts with that of classic ecological models such as those for predator and prey systems that are characterized by negative feedback and can exhibit more complex dynamics than equilibria such as oscillations, periodic-doubling bifurcations, and chaos. To understand the basic mechanisms of feedbacks in the coupled systems, consider, for example, a simple predator-prey model of the form: $\dot{x} = U(x, z), \dot{z} = V(x, z)$, where x is the prey and z is the predator. Because the predator reduces prey density or biomass, $U_z(x, z) < 0$, and because the prey leads to an increase in the predator density or biomass, $V_x(x, z) > 0$, so that the product, $U_z(x, z)V_x(x, z) < 0$, where U_z denotes the partial derivative of U with respect to z and V_x denotes the partial derivative of V with respect to x. The product $U_z(x, z)V_z(x, z) < 0$, conveys negative feedback throughout the state space. In contrast, for our simplest model ((i) in Table 2 of the manuscript), the product, $U_I(h, I)V_h(h, I) \geq 0$, and thus the system is characterized by positive feedback throughout the state space. This basic relationship can be extended to systems with multiple dimensions of capital and natural enemies, where capital is defined as a state variable that complements other state variables for the production of income, and natural enemies are defined as state variables that reduce capital. More generally, members within each group all complement

one another but the members of two different groups are individually and so collectively antagonistic to one another: i.e., friends of friends are friends, friends of enemies are enemies, and enemies of enemies are friends. To illustrate this, consider the matrix

$$\begin{pmatrix} J_{aa} & J_{ab} & J_{ac} & -J_{ad} & -J_{ae} \\ J_{ba} & J_{bb} & J_{bc} & -J_{bd} & -J_{be} \\ J_{ca} & J_{cb} & J_{cc} & -J_{cd} & -J_{ce} \\ -J_{da} & -J_{db} & -J_{dc} & J_{dd} & J_{de} \\ -J_{ea} & -J_{eb} & -J_{ec} & J_{ed} & J_{ee} \end{pmatrix},$$

representing the Jacobian (array of partial derivatives) of a prototypical monotone dynamical system within the framework of the general model (Equations (1)-(2)), where $J_{ij} \geq 0, i, j \in \{a, b, c, d, e\}$, with the subscripts denoting state variables. In this example, there are two mutually antagonistic groups, the first consisting of three types of capital and the second consisting of two types of natural enemies to capital. The $J'_{ii}s, i \in \{a, b, c, d, e\}$ represent indeterminacy in that, to result in monotonicity, nothing is actually required of the effect of a factor on itself.

More formally, given capital variables, $\mathbf{x} = (x_1, x_2, x_3, \ldots, x_M)$ in one group and "natural enemies of capital" $\mathbf{z} = (z_1, z_2, z_3, \ldots, z_J) = (x_{n+1}, x_{n+2}, x_{n+3}, \ldots, x_J)$ in a second group, then for dynamics described by the system of equations $\dot{\mathbf{X}} = \mathbf{F}(\mathbf{X})$, where $\mathbf{X} = (\mathbf{x}, \mathbf{z})$, the necessary condition for a monotone system is:

$$\frac{\partial F_i(\mathbf{X})}{\partial x_j} \leq 0, \text{ or } \frac{\partial F_i(\mathbf{X})}{\partial x_j} \geq 0, \ \forall i \neq j, \ i = 1, 2, 3, \ldots, M, \ j = n+1, n+2, n+3, \ldots, J.$$

In such monotone systems, the only attractors are stable equilibria: there are no limit cycles or complex dynamics such as period-doubling bifurcations, chaos, etc. As a specific example, the explicit Jacobian matrix for model (i) in Table 2 of the main article is:

$$\begin{pmatrix} J_{hh} & -J_{hI} \\ -J_{Ih} & J_{II} \end{pmatrix},$$

where $J_{hI} = -mr_h(1-I^*)^{m-1}{h^*}^{\alpha_h}, \ \ J_{hI} = -\frac{\alpha_h \phi \gamma_{min} \gamma_y (\gamma_y - 1) I^* {h^*}^{\alpha_h - 1}}{({h^*}^{\alpha_h} + \gamma_y)^2}$. If (h^*, I^*) is an equilibrium state of model (i), then $U_I(h^*, I^*) = -mr_h(1-I^*)^{m-1}{h^*}^{\alpha_h} < 0, U_h(h^*, I^*) = -\frac{\alpha_h \phi \gamma_{min} \gamma_y (\gamma_y - 1) I^* {h^*}^{\alpha_h - 1}}{({h^*}^{\alpha_h} + \gamma_y)^2} \leq 0$, and $U_I U_h \geq 0$.

As another example, consider system (iii) in Table 2 of the main article:

$$\begin{pmatrix} J_{kk} & J_{kh} & -J_{kI} \\ J_{hk} & J_{hh} & -J_{hI} \\ -J_{Ik} & -J_{Ih} & J_{II} \end{pmatrix}, \text{where}$$

$$\begin{aligned}
J_{kh} &= r_k\alpha_h(1-\xi I)^m y h^{-1}, \quad J_{kI} = r_k m(2-\alpha_h-\alpha_k)\xi(1-\xi I)^{-1}y, \\
J_{hk} &= r_h\alpha_k(1-\xi I)^m y k^{-1}, \quad J_{hI} = r_h m(2-\alpha_h-\alpha_k)\xi(1-\xi I)^{m-1}y, \\
J_{Ih} &= \left(\frac{\beta_{max}\beta_y\alpha_h(1-I)Iy}{(y+\beta_y)^2 h} + \frac{\alpha_h\gamma_{min}\gamma_y(\gamma_y-1)Iy}{(y+\gamma_y)^2 h}\right), \\
J_{Ik} &= \left(\frac{\beta_{max}\beta_y\alpha_k(1-I)Iy}{(y+\beta_y)^2 k} + \frac{\alpha_k\gamma_{min}\gamma_y(\gamma_y-1)Iy}{(y+\gamma_y)^2 k}\right).
\end{aligned}$$

The two forms of capital, k and h, complement each other; in addition, each of them negatively affects disease transmission and disease levels in turn negatively affect each of them. Clearly, $J_{ij} \geq 0, \forall i \neq j$ and $\gamma_y \geq 1$.

This general class of monotone systems have no attractors other than stable equilibria, and in the case of strong positive feedback, there can be two stable equilibria. In contrast to variants of the simple economic-disease system, which can be shown to exhibit positive feedback across the capital-disease space, the directions of feedback of the renewable resources and their natural enemies are ambiguous, and therefore the system is not necessarily monotone. In the third differential equation of systems (iv) and (v), for example, capital increases the carrying capacity of the resource, but also increases the harvesting rate, thus exhibiting mechanisms of both positive and negative feedback. While these systems can potentially exhibit more complex dynamics, such as periodic cycles and chaos, no such dynamics were observed in our models. Due to the complexity of most of the coupled systems, it is challenging if not impossible to study their dynamics analytically. Thus, we resort to numerical analyses. There are two main goals for the analyses: 1) to determine the plausibility of poverty traps, by identifying the portion of the feasible parameter space that generates the different development regimes (globally stable development, globally stable poverty, and bistability), and 2) to identify the specific parameters to which the dynamics of the systems are most sensitive. Before describing the methods for these two main objectives, we include specific bifurcation analyses

for some of the systems, to complement those in the main text.

S3.2 Analysis of the basic coupled model with no population growth

For heuristic purposes, Fig. S4 presents bistability conditions for Model (i) (Table 2) by analyzing outcomes over portions of the parameter space. In Fig. S4(a) the dashed blue line represents a system with no disease feedback ($m = 0$), equivalent to the neoclassical growth model in economics. Above a certain number of pathogens, this system is characterized by a globally stable equilibrium. As labor productivity decreases with disease prevalence and the number of pathogens in the population, capital depreciation may exceed capital accumulation at low levels of income and the system becomes bistable. In this case, the final outcome is contigent to history. Figure S4(a) thus shows how the classical poverty trap model can be derived from our general framework, which is also presented using a different production function in Ngonghala et al.[23]. The nonlinearity in the capital accumulation (respectively, income) curve emerges due to reinforcing feedbacks in disease transmission and recovery: at high numbers of pathogens, low initial income levels are associated with high disease exposure and low recovery rates (e.g., due to poor nutrition or lack of health care), which decreases labor productivity and human capital accumulation, causing a "vicious cycle". As initial income levels rise, disease transmission falls and the recovery rate rises for all pathogens in the system, creating a positive feedback that eventually leads to healthy economic growth (the capital accumulation curve to rise above depreciation). Figure S4(b)-(c) presents different development regimes that result from different combinations of the capital investment rate r_h, and the capital depeciation rate δ_h. It shows how the region of bistability denoted by II grows with the number of the pathogens m, in the system.

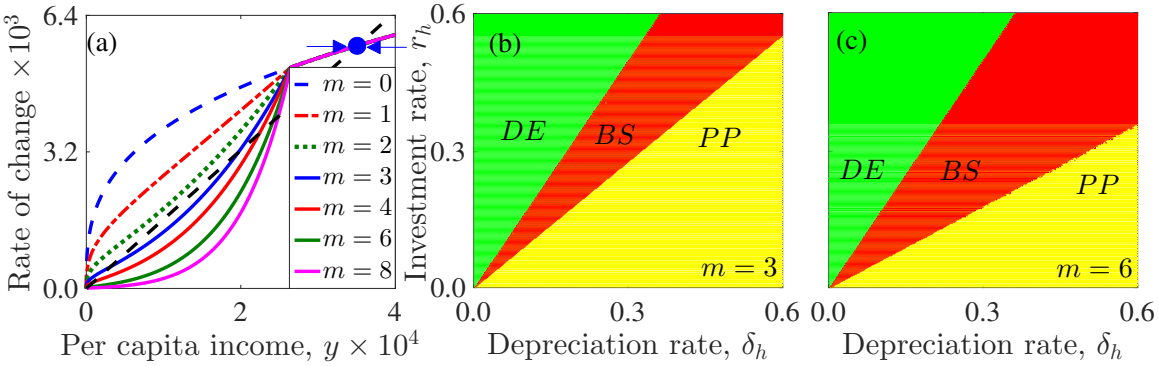

Figure S4: Multiple infections create poverty traps. (a) The effects of multiple diseases on the dynamics of income for the one-dimensional model version of model (i), i.e., Equation (S15). The straight dash-black line is the depreciation term. All other lines represent accumulation terms. When the number of diseases is small, capital accumulation exceeds depreciation, near the origin, and there is only one stable equilibrium (first three accumulation curves). However, as the number of pathogens rises, the accumulation term falls nonlinearly below the depreciation term (solid accumulation curves), creating bistability, and hence poverty traps. (b)-(c) Bistability regions for various combinations of the capital investment rate r_h, and the capital depreciation rate δ_h, when there are three and six diseases in the system. The green area denoted by DE indicates parameter values for which there is only a globally stable development equilibrium, the yellow area denoted by PP indicates the parameter space that generates only a stable poor equilibrium (persistent poverty), and the red area labeled BS indicates the parameters that generate bistable outcomes.

To understand the impact of various parameters on the equilibrium properties, we conducted a local sensitivity analysis in which all but one of the parameters of the Model (i) are fixed to their original calibration, while one parameter is varied. The blue and dashed red curves in Fig. S5(a)-(c) represent stable and unstable equilibria. Consider for example, Fig. S5(c) and the minimum recovery rate from infection, γ_{min}. For values of γ_{min} below a threshold, $R_0 > 1$, and the endemic equilibrium is high. As γ_{min} rises past this first threshold, there is a phase transition to two stable equilibria–an infection-free equilibrium (the "development"equilibrium) and an endemic disease burden equilibrium (the poverty trap). After a second threshold, the system converges to only a single globally stable equilibrium (low disease and high income).

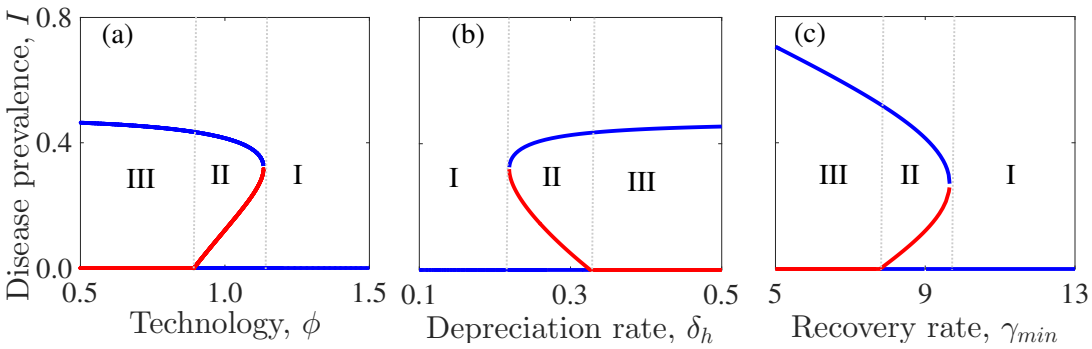

Figure S5: Local sensitivity analysis of disease prevalence to the technological progress ϕ, capital depreciation rate δ_h, and minimum recovery rate from disease γ_{min}, for the basic coupled disease-economic model (i) showing bounds on the parameters for which bistability occurs. Blue lines denote stable equilibria, while red lines denote unstable equilibria. Bistability occurs within region II (demarcated by dotted gray vertical lines), and for intermediate values of the parameters. Persistent poverty occurs within region III, while there is globally stable development in region I.

S3.3 Analysis of extended models

Three-dimensional bifurcation time evolution dynamics of Models (iv'), (ix), and (x) in Table S1 are presented in Fig. S6. For small maximum consumption rate of plants by pests b_{max} (Fig. S6 (a)) and for small maximum disease transmission rates β_{max} (Fig. S6 (b)-(c)), the system experiences global development (high per capita income and low disease) and trajectories from different initial per capita income and disease prevalence levels relax on this globally stable equilibrium. At the first threshold maximum plant consumption and disease transmission rates, the system bifurcates into two stable equilibria (a development and a poverty trap equilibrium). Trajectories originating from the basin of attraction of the development equilibrium converge to the development equilibrium, while trajectories originating from the basin of attraction of the poverty trap converge to the poverty equilibrium. At the second threshold maximum plant consumption and disease transmission rates, the system experiences global persistent poverty (low per capita income and high disease burden) and trajectories originating from different starting points settle on this equilibrium.

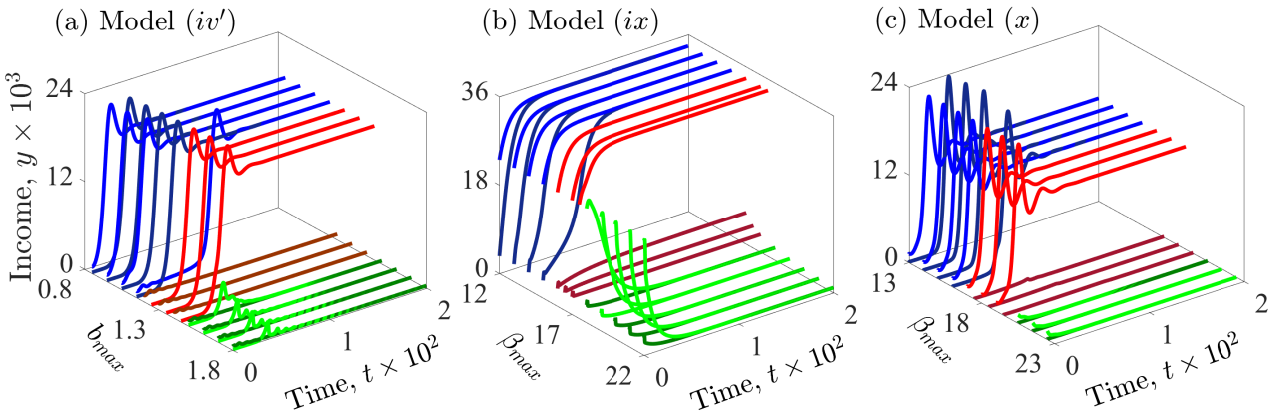

Figure S6: Dynamics of per capita income for the coupled ecological-economic models. Bifurcation diagram showing the time path evolution from two initial per capita income values (denoted by light and dark colors) as the maximum plant consumption rate by pests b_{max} changes ((a)) and as the maximum disease transmission rate, β_{max}, changes ((b)-(c)). (a) corresponds to Model (iv'), (b) corresponds to Model (ix), (c) corresponds to Model (x). Light and dark blue lines converge to a globally stable development equilibrium (high income and low disease) in the long-run, light and dark green lines converge to globally stable poverty trap (low income and high disease) in the long-run and the red lines depict trajectories within the region of bistability (light and dark red trajectories settle at different points: low income and high disease for the poverty equilibrium and high income and low disease for the development equilibrium). (b)-(c): As β_{max} increases, the system bifurcates from a single stable development equilibrium (blue trajectories) through bistability (red trajectories) to a single stable persistent poverty equilibrium (green trajectories).

S4 Global uncertainty and sensitivity analysis

The global uncertainty and sensitivity analysis is performed in accordance with the Latin Hyper-cube Sampling (LHS) and Partial Rank Correlation Coefficient (PRCC) methods[36]. In each case, we treat the estimated or baseline parameters as mean values and build a feasible range for each parameter with minimum and maximum values corresponding to those in the literature. Where we could not find minimum and maximum values of the parameters in the literature, we set these limits to $\pm 50\%$ of the mean, while ensuring that the range is feasible. Since the distributions of the parameters are unknown, we assume for simplicity a uniform distribution between the minimum and maximum values of each parameter. We then sample parameter sets randomly with no replacement from their distributions and construct a matrix whose rows are made up of different sets of parameters. Each of these parameter regimes is used to simulate the coupled system

under consideration. The parameters and outputs, e.g., disease prevalence at equilibrium, per capita income equilibrium, renewable resource density at equilibrium, percentage of trajectories converging to the poverty trap or development equilibrium, etc. are then ranked and PRCCs together with corresponding p-values to investigate whether the PRCCs are statistically significant, i.e., differ significantly from zero are computed. See References[36–38] for details on how to compute the PRCCs. We use the computed PRCCs to assess the sensitivity of model outputs to variations in model parameters. The PRCCs establish the correlation or how strongly model inputs (parameters) are related to specific outputs of the model. They range in value from -1 to 1, with a magnitude of 1 depicting a perfect correlation between a parameter and an output; i.e., the parameter influences the output most, while a PRCC value of 0 depicts no correlation between a parameter and an output; i.e., the parameter has no influence on the output. A positive PRCC indicates that the output increases with increasing values of the parameter under consideration, while a negative PRCC indicates that increasing a parameter will trigger a decline in model output. Since the use of PRCCs relies on the existence of monotonic relationships between model outputs, e.g., disease prevalence and income, and model inputs, e.g., model parameters, we carried out another analysis to ascertain this. An illustration for disease prevalence and income against key parameters such as the maximum transmission rate, minimum recovery rate and elasticity coefficient for the basic model is presentd in Fig. S8. Finally, although this sensitivity analysis approach identifies the parameters which contribute most to output variability, it does not quantify the exact amount of variability.

To quantify the size of the bistability region, we repeat the above global sensitivity analysis exercise but for each of the sampled set of parameters, the system is simulated for 100 randomly selected initial conditions also assembled through the LHS technique. We then determine whether the system converges to a globally stable development or poverty equilibrium or whether multiple locally stable equilibria coexist for a specific combination of parameters. See Fig. 3 in the main text.

We further identify important parameters that drive the outputs of the coupled systems, including

equilibrium disease prevalence and income, as well as the percentage of trajectories that converge to the poverty trap and development equilibrium within the bistability parameter regime. Figure S7 shows how influential various model parameters are to infectious disease prevalence and the percentage of trajectories that converge to the poverty trap within the bistability parameter regime for models (i), (iii) and (iv), while Fig. S9 illustrates the influence of parameters to per capita income and infectious disease prevalence for Model (vi). In all models involving human diseases, uncertainty of variability in the maximum human disease transmission rate, β_{max}, and the minimum recovery rate from human infections, γ_{min} will introduce the greatest uncertainty or variability in disease prevalence, per capita income or the percentage of trajectories converging to the poverty trap with the bistability region. The number of pathogens in the system, m, is also important in generating uncertainty or variability in per capita income. Overall, both ecological and economic parameters are important in determining the size of the bistability region, but epidemiological parameters like β_{max} and γ_{min} are more influencial.

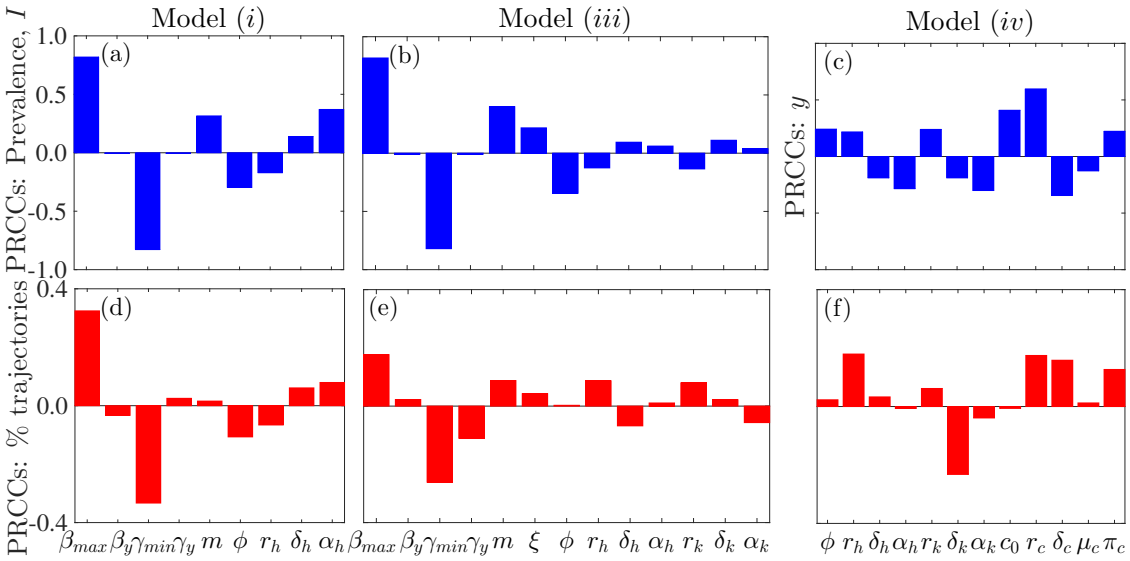

Figure S7: Partial rank correlation coefficients (PRCCs) depicting the contributions of parameters to disease prevalence ((a)-(b)) for models (i) and (iii), per capita income ((c)) for model (iv) and the percentage of trajectories converging to the poverty trap within the bistability region ((d)-(f)) for Systems (i), (iii) and (iv). The larger the magnitude of the PRCC, the more significant the parameter is in generating uncertainty or variability in the output. The sign of the PRCC, i.e., positive or negative, indicates whether an increase in a parameter will lead to an increase (when it is positive) or decrease (when it is negative) in the output.

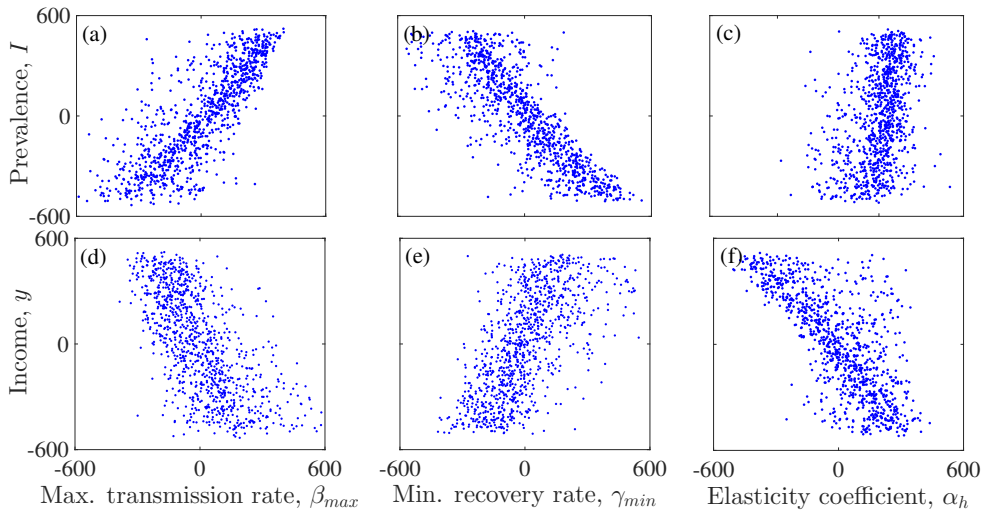

Figure S8: Plots depicting monotonic relationships between infectious disease prevalence and income against some key parameters of System (i).

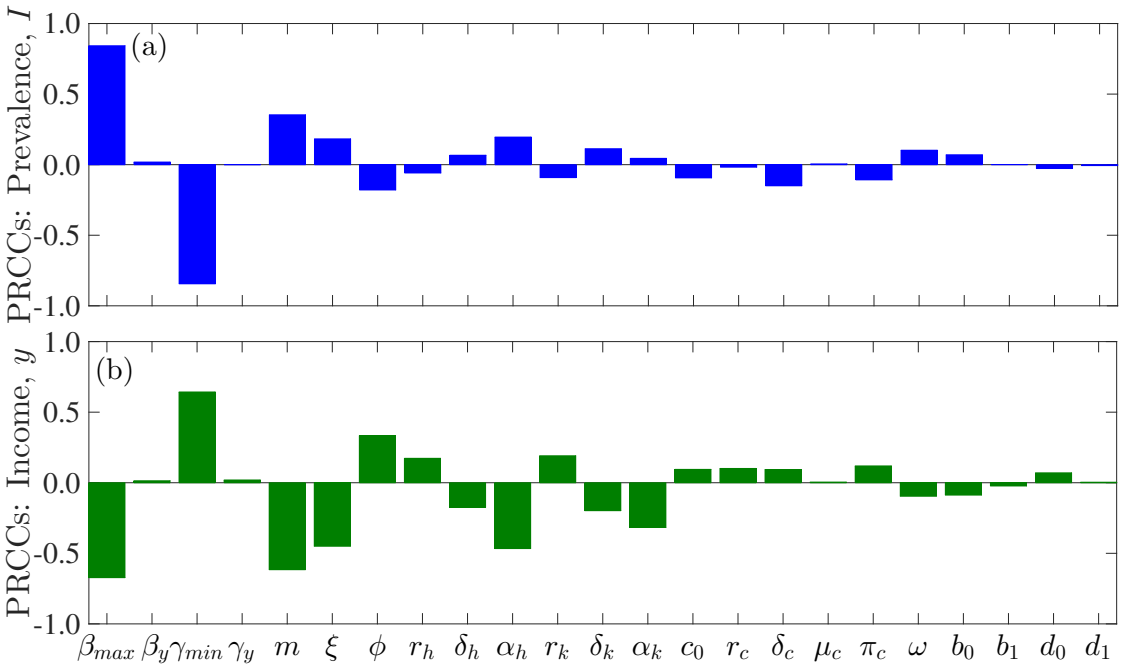

Figure S9: Partial rank correlation coefficients (PRCCs) depicting the significance of parameters to per infectious disease prevalence and capita income for System (vi).

S5 Limitations

Although in this manuscript, we used ordinary differential equations as the main mathematical modeling tool, other approaches might also be employed depending on the question, availability/type of data, and how much one would benefit in terms of knowledge and tractibility when more realism and hence complexity is introduced. Statistical models, e.g., regressions and time series analyses will be appropriate for somebody who is interested in exploring correlations and patterns in data, while dynamical models, e.g., determinsitic (including the one we have proposed here), stochastic, network, agent-based models will be more useful to people who intend to simulate processes that evolve with time. Introducing additional disease classes, e.g., exposed and recovery classes may be important for people who are interested in diseases with long incubation periods live HIV and diseases that confer permanent immunity like measles. The use of stochastic and individual-based models may be unavoidable when the population sizes under consideration are small.

S6 Code and data availability

S6.1 Code availability

All the models in the main text and the SI were analyzed using MATLAB version R2015a. All the codes can be made available upon request (send an email to calistusnn@ufl.edu).

S6.2 Data availability

No datasets were generated or analysed during the current study.

1. Lotka, A. Contribution to the theory of periodic reaction. *Journal of Physical Chemistry* **14 (3)**, 271–274 (1910).

2. Bailey, T. J. N. *The mathematical theory of infectious diseases and its application* (Griffin, London,

1975), 2nd edn.

3. Hethcote, H. Qualitative analyses of communicable disease models. *Mathematical Biosciences* **28**, 335–356 (1976).

4. Anderson, R. & May, R. *Infectious diseases of humans: dynamics and control* (Oxford University Press, New York, NY, 1992).

5. Keeling, M. J. & Rohani, P. *Modelling infectious diseases* (Princeton University Press, Princeton, NJ, 2007).

6. Ngonghala, N. Calistus, Mohammed-Awel, Jemal, Zhao, Ruijun & Prosper, Olivia Interplay between insecticide-treated bed-nets and mosquito demography: implications for malaria control. *Journal of Theoretical Biology* **397**, 179–192 (2016).

7. Diekmann, O., Heesterbeek, J. A. P. & Metz, J. A. J. On the definition and computation of the basic reprodcution ratio R_0 in models for infectious diseases in heterogeneous populations. *Journal of Mathematical Biology* **28**, 365–382 (1990).

8. van den Driessche, P. & Watmough, J. Reproduction numbers and sub-threshold endemic equilibria for compartmental models of disease transmission. *Mathematical Biosciences* **180**, 29–48 (2002).

9. Noy-Meir, I. Stability of grazing systems: an application of predator-prey graphs. *The Journal of Ecology* **63**, 459–481 (1975).

10. van de Koppel, J., Rietkerk, M. & Weissing, F. J. Catastrophic vegetation shifts and soil degradation in terrestrial grazing systems. *Trends in Ecology & Evolution* **12**, 352–356 (1997).

11. Rietkerk, M. & Van de Koppel, J. Alternate stable states and threshold effects in semi-arid grazing systems. *Oikos* 69–76 (1997).

12. Verhulst, P. F. Recherches mathématiques sur la loi d'accroissement de la population. *Nouveaux Mémoires de l'Académie Royale des Sciences et Belles-Lettres de Bruxelles* **18**, 14–54 (1845).

13. Eberhardt, L., Breiwick, J. & Demaster, D. Analyzing population growth curves. *Oikos* **117**, 1240–1246 (2008).

14. Volterra, V. Variazioni e fluttuazioni del numero dindividui in specie animali conviventi. *Mem. Acad. Lincei Roma* **2**, 31–113 (1926).

15. Hillier, J. G. & Birch, A. N. E. A bi-trophic mathematical model for pest adaptation to a resistant crop. *Journal of Theoretical Biology* **215**, 305–319 (2002).

16. Nisbet, R. M. & Gurney, W. S. C. *Modelling Fluctuating Populations* (John Wiley and Sons, London, 1982).

17. Solow, R. A contribution to the theory of economic growth. *The quarterly journal of economics* **70 (1)**, 65–94 (1956).

18. Cobb, C. W. & Douglas, P. H. A theory of production. *The American Economic Review* **18**, 139–165 (1928).

19. Mankiw, N., Romer, D. & Weil, D. A contribution to the empirics of economic growth. *The quarterly journal of economics* **107**, 407–437 (1992).

20. Azariadis, C. & Stachurski, J. Poverty traps. *Handbook of economic growth* **1**, 295–384 (2005).

21. Sachs, J. *et al.* Ending Africa's poverty trap. *Brookings papers on economic activity* **2004 (1)**, 117–240 (2004).

22. Durlauf, S. N. A theory of persistent income inequality. *Journal of Economic Growth* **1**, 75–93 (1996).

23. Ngonghala, C. N. *et al.* Poverty, disease, and the ecology of complex systems. *PLoS Biology* **12 (4)**, e1001827 (2014).

24. Stevens, P. 4 diseases of poverty and the 10/90 gap. *International policy network* (2004).

25. UN Panel Report. Poverty, infectious disease, and environmental degradation as threats to collective security. *Population and development review* **31 (3)**, 595–600 (2005).

26. Miguel, E. & Kremer, M. Identifying impact on education and health in the presence of treatment externalities. *Econometrica* **72**, 159–217 (2004).

27. Bleakley, H. Disease and development: evidence from hookworm eradication in the american south. *Quarterly Journal of Economics* **122**, 73–117 (2007).

28. Arrow, K. J., Chenery, H. B., Minhas, B. S. & Solow, R. M. Capital-labor substitution and economic efficiency. *The Review of Economics and Statistics* **43**, 225–250 (1961).

29. Fisher, R. A. *et al.* A mathematical examination of the methods of determining the accuracy of an observation by the mean error, and by the mean square error. *Monthly Notices of the Royal Astronomical Society* **80**, 758–770 (1920).

30. Myung, I. J. Tutorial on maximum likelihood estimation. *Journal of Mathematical Psychology* **47**, 90–100 (2003).

31. Murray, C. J. L. & Lopez, A. D. *Global burden of disease: a comprehensive assessment of mortality and disability from diseases, injuries, and risk factors in 1990 and projected to 2020* (Harvard University Press, Cambridge MA, 1996).

32. Lopez, A. D., Mather, C. D., Ezzati, M., Jamison, D. T. & L, M. C. J. *Global burden of disease and risk factors* (Oxford University Press, New York, NY, 2006).

33. World Bank Development Data Group. World development indicators online. *The World Bank (http://go.worldbank.org/3JU2HA60D0)* (2007).

34. Central Intelligence Agency. Country comparison: birth rate. *The world fact book* (2015).

35. Central Intelligence Agency. Country comparison: life expectancy at birth. *The world fact book* (2015).

36. Marino, S., Hogue, I., Ray, C. & Kirschner, D. A methodology for performing global uncertainty and sensitivity analysis in systems biology. *Journal of Theoretical Biology* **254**, 178–196 (2008).

37. Blower, S. & Dowlatabadi, H. Sensitivity and uncertainty analysis of complex models of disease transmission: an hiv model, as an example. *International Statistical Review/Revue Internationale de Statistique* 229–243 (1994).

38. Wu, J., Dhingra, R., Gambhir, M. & Remais, J. V. Sensitivity analysis of infectious disease models: methods, advances and their application. *Journal of The Royal Society Interface* **10**, 20121018 (2013).

Correspondence Correspondence and requests for materials should be addressed to Calistus N. Ngonghala (email: calistusnn@ufl.edu).